On the evolution of the velocity gradient tensor in transitional boundary layers

By A. Elnahhas, P. L. Johnson, A. Lozano-Durán AND P. Moin

1. Motivation and objectives

The transition of a boundary layer from a laminar to a turbulent state is associated with a rapid increase in the friction and heat transfer coefficients due to the enhanced mixing caused by turbulence. This transition is accompanied by the rapid growth of velocity gradients throughout the boundary layer, which can be appreciated by visualizing isosurfaces of the Q-criterion or other vortex identifiers and is particularly evident in late-stage transition, when growing structures abruptly break down into more chaotic flow, generating turbulent spots (Wu *et al.* 2017). This drastic change is important from both the applied and fundamental points of view. In this report, we approach the transition problem by studying the dynamics of the velocity gradient tensor.

Canonical transition from laminar to turbulence is conceptually divided into several steps: the receptivity process, in which the perturbations are introduced into the boundary layer (for example, by Tollmien-Schlichting (TS) wave modes), followed by a primary instability, nonlinear saturation resulting in a new base state, secondary instability, and eventually breakdown into turbulence (Schmid & Henningson 2001). In the first steps, linear stability analysis predicts the unstable nature of the laminar boundary layer profile. Local stability analysis of the linearized Navier-Stokes equations leads to the emergence of two-dimensional waves, which grow exponentially in time (Mack 1984). These TS waves modulate the base flow of the laminar boundary layer and grow to a finite amplitude, which gives rise to a new base state. The linear analysis of this new base state is typically framed as a secondary instability. This results in various types of transition mechanisms, depending on whether the secondary instability has the same fundamental frequency as the TS wave or is a subharmonic of that frequency, respectively called K-type and H-type instabilities (Herbert 1988).

Most linear stability analyses deal with solutions which are exponentially growing in either space or time. This exponential growth continues until nonlinear mechanisms become important and saturate the amplitude of the unstable modes before the breakdown occurs. Hence, linear stability analysis does not characterize the saturation process. In the present brief, we propose to study the velocity gradient tensor to characterize the late nonlinear stages of transition.

In the fully turbulent regime, the Lagrangian dynamics of the velocity gradient tensor have been studied extensively in canonical scenarios from homogeneous isotropic turbulence (HIT) to turbulent boundary layers. The governing equations of the velocity gradient tensor are directly derived from the Navier-Stokes equations. In the seminal works of Vieillefosse (1982) and Cantwell (1992) a simplified version of the equations, in which the nonlocal contributions of pressure and viscosity are neglected, was solved analytically. This simplified restricted Euler system reproduces frequently observed features in direct numerical simulation (DNS) databases of simple turbulent flows and high-dissipation regions of complex turbulent flows. These features include the positivity and small value

of the intermediate strain rate eigenvalue, as well as the alignment of the vorticity vector with the intermediate eigenvector of the strain rate (Ashurst *et al.* 1987). The analysis of the evolution of the velocity gradient tensor can be recast in the form of its invariants, Q and R, which represent the balance between rotation- and strain rate production-dominated regions, respectively. When the restricted Euler system is recast in this form, it provides an insightful picture of the topological states through which a Lagrangian fluid particle could evolve.

In this preliminary study, we are interested in quantifying the growth of velocity gradients as a function of the downstream coordinate, along with the dominant terms that lead to this growth at each stage of the boundary layer. It will also be shown that the balance of enstrophy production and viscous dissipation presented by Tennekes & Lumley (1972), valid at high Reynolds numbers, also holds immediately after transition. To quantify the streamwise growth of velocity gradients, several scalar quantities are considered from an Eulerian budget point of view for a zero-pressure-gradient flat-plate boundary layer. This analysis is carried out using a DNS data of H-type transition. It is argued that, based on the modeling experience of the nonlocal pressure and viscous terms in homogeneous turbulence, the budget which exhibits the least streamwise pressure dependence should be pursued further, due to the potential of easier modeling in subsequent works.

The remainder of this report is structured as follows. Section 2 presents the argument behind why the Frobenius norm of the velocity gradient tensor is chosen to be analyzed, along with the derivation of its spanwise/temporally averaged Eulerian streamwise budget. Section 3 describes the numerical framework used to generate the DNS database, along with the results of computing the budget presented in Section 2. Finally, conclusions are presented in Section 4.

2. Eulerian streamwise velocity gradient tensor budget equations

Consider the incompressible Navier-Stokes equations,

$$\frac{\partial u_i}{\partial t} + u_j \frac{\partial u_i}{\partial x_j} = -\frac{\partial p}{\partial x_i} + \nu \frac{\partial^2 u_i}{\partial x_j \partial x_j}, \tag{2.1}$$

where u_i is the velocity component in the ith direction, $x, y,$ and z are the streamwise, wall-normal, and spanwise directions, respectively, ν is the kinematic viscosity, and p is the kinematic pressure. The frame of reference adopted in the subsequent analysis is the one fixed to the origin of the boundary layer. Taking the gradient of Eq. (2.1) leads to a governing equation for the velocity gradient tensor,

$$A_{ij} = \frac{\partial u_i}{\partial x_j}. \tag{2.2}$$

The equation for its evolution is given by

$$\frac{\partial A_{ij}}{\partial t} + u_k \frac{\partial A_{ij}}{\partial x_k} = -A_{ik} A_{kj} - \frac{1}{\rho} \frac{\partial^2 p}{\partial x_i \partial x_j} + \nu \frac{\partial^2 A_{ij}}{\partial x_k \partial x_k}, \tag{2.3}$$

where we follow the nomenclature by Meneveau (2011). From a Lagrangian perspective, Eq. (2.3) is not closed in terms of A_{ij} at position $\vec{x}$ and time t due to the last two terms on the right-hand side, those being the pressure Hessian and the viscous terms. Taking the trace of Eq. (2.3) while accounting for the incompressibility condition $A_{ii} = 0$ leads

to the Poisson equation for pressure

$$\frac{\partial^2 p}{\partial x_l \partial x_l} = -A_{lk}A_{kl}, \tag{2.4}$$

which can be used to separate the local and nonlocal parts, in a Lagrangian manner, of Eq. (2.3) as follows

$$\frac{\partial A_{ij}}{\partial t} + u_k \frac{\partial A_{ij}}{\partial x_k} = -(A_{ik}A_{kj} - \frac{1}{3}A_{mk}A_{km}\delta_{ij}) + H^p_{ij} + H^\nu_{ij}, \tag{2.5}$$

where

$$H^p_{ij} = -\left(\frac{\partial^2 p}{\partial x_i \partial x_j} - \frac{1}{3}\frac{\partial^2 p}{\partial x_k \partial x_k}\delta_{ij}\right) \text{ and } H^\nu_{ij} = \nu \frac{\partial^2 A_{ij}}{\partial x_k \partial x_k}, \tag{2.6}$$

are the anisotropic part of the pressure Hessian and the viscous term, respectively.

In this report, we are interested in characterizing the growth of the velocity gradients in an aggregate manner as a function of the downstream coordinate. We aim at identifying a scalar quantity which to characterize nonlinear stages of transition. To this end, it is possible to derive the evolution equation of several scalar quantities by making appropriate contractions between various terms and Eq. (2.5). The resulting equations are then averaged along the homogeneous directions and in time, then integrated across the boundary layer thickness to establish the Eulerian streamwise budgets.

It is beneficial for these quantities, along with their governing equations, to possess certain properties. First, the statistical mean of the quantity being examined needs to be appreciably different in the laminar and turbulent regions of the flow. Second, the terms contributing to the growth or decay of this quantity should be physically interpretable to elucidate the processes at place. Third, and perhaps with a more practical outlook in mind, the dominant terms responsible for the growth and decay of the selected quantity should be amenable to modeling. The following subsections discuss possible candidates for quantities to be used as transition markers.

2.1. *The Q equation*

Contracting Eq. (2.5) with the transpose of the velocity gradient tensor A_{ji} yields the evolution equation for the second invariant of the velocity gradient tensor

$$\frac{\partial Q}{\partial t} + u_k \frac{\partial Q}{\partial x_k} = -3R - A_{ji}H^p_{ij} - A_{ji}H^\nu_{ij}, \tag{2.7}$$

where

$$Q = -\frac{1}{2}A_{im}A_{mi} = \frac{1}{2}(\Omega_{im}\Omega_{im} - S_{im}S_{im}) \text{ and } R = -\frac{1}{3}A_{im}A_{mn}A_{ni}, \tag{2.8}$$

are the second and third invariants of the velocity gradient tensor. Ω_{ij} and S_{ij} are the rotation and strain rate tensors, respectively. Regions of high Q are rotation dominated, and regions of high R are strain production dominated.

From the perspective of the Eulerian budgets discussed above, Q is not a good indicator for transition. Consider the case of statistically stationary, homogeneous turbulence. $\overline{Q}$, where the overbar denotes averaging in the homogeneous directions and in time, is a function of only the mean velocity gradients, and as such, its expectation is zero for most homogeneous flows, indicating that the contribution of rotation- and strain- dominated regions to an integral measure based on $\overline{Q}$ will balance. This approximately holds at high Reynolds numbers in a turbulent boundary layer. In the laminar region of a boundary

layer, $\overline{Q}$ is of the same order of magnitude as that found in the turbulent region; therefore, there is no differentiation between the two cases when considering the evolution of an integral quantity based on Q. Furthermore, the viscous term in Eq. (2.7) can be rewritten to have a term akin to dissipation in the kinetic energy equation

$$\nu \frac{\partial A_{ij}}{\partial x_k} \frac{\partial A_{ji}}{\partial x_k}, \tag{2.9}$$

which cannot be associated with a particular sign and is, therefore, lacking physical interpretability. Thus, an equation based on Q does not satisfy two of the three properties outlined above. In order to remedy these two deficiencies, we consider the evolution equations for Q^2 and the Frobenius norm of the velocity gradient tensor, $|A|_F^2 = A_{ij}A_{ij}$.

2.2. *The Q^2 equation*

It has been argued that looking at an integral quantity based on $\overline{Q}$ in a boundary layer would not provide a contrasting view between the laminar and turbulent portions. In contrast, it is apparent that rotating and straining regions are ubiquitous in the turbulent boundary layer compared to the laminar one. As such, an integral measure that sums up the contributions of both rotation- and strain-dominated regions could differentiate between the laminar and turbulent regions. Therefore, let us consider the evolution equation for Q^2. By contracting Eq. (2.7) with Q, we get

$$\frac{\partial Q^2}{\partial t} + u_k \frac{\partial Q^2}{\partial x_k} = -6QR - 2Q(A_{ji}H_{ij}^p + A_{ji}H_{ij}^\nu), \tag{2.10}$$

which possesses a positive source term in the mean because one can see that Q and R are negatively correlated by looking at their characteristic teardrop-shaped joint probability distribution function (Soria *et al.* 1994).

Even though considering $\overline{Q^2}$ alleviates the problem associated with $\overline{Q}$ having a similar value in the laminar and turbulent portions of a boundary layer, a problem with the pressure term arises. The pressure term in Eq. (2.10), after the streamwise budget equation for $\overline{Q^2}$ is formulated, involves a correlation between Q and the divergence of the velocity and pressure gradients. Through numerically analyzing the $\overline{Q^2}$ budget, it is found that this correlation is a dominant term. Recalling that the anisotropic portion of the pressure Hessian leads to a closure problem from a Lagrangian perspective, many attempts have been made at modeling its effect. In HIT, examples of these models include the tetrad model by Chertkov *et al.* (1999) and the fluid deformation approximation by Chevillard & Meneveau (2006). However, unlike the viscous term, which acts to damp all the trajectories in the Q and R phase space by driving them toward the origin, the effect of the deviatoric part of the pressure Hessian differs depending on the region of the Q and R phase space being examined (Chevillard *et al.* 2008). This difficulty associated with modeling the pressure Hessian in HIT is expected to be exacerbated when transition in a boundary layer is considered. Since we are examining a zero-pressure-gradient flat-plate boundary layer, and keeping these future modeling difficulties in mind, a governing equation that allows for the neglect of the pressure term is pursued.

2.3. *The $|A|_F^2$ equation*

Contracting Eq. (2.5) with the velocity gradient tensor A_{ij} itself leads to

$$\frac{\partial |A|_F^2}{\partial t} + u_k \frac{\partial |A|_F^2}{\partial x_k} = -2A_{ik}A_{kj}A_{ij} + 2A_{ij}H_{ij}^p + 2A_{ij}H_{ij}^\nu, \tag{2.11}$$

where $|A|_F^2 = A_{ij}A_{ij}$. The pressure Hessian and the viscous terms in Eq. (2.11) can be written in the following form

$$\frac{\partial |A|_F^2}{\partial t} + u_k \frac{\partial |A|_F^2}{\partial u_k} = -2A_{ik}A_{kj}A_{ij} - 2\frac{\partial}{\partial x_i}\left(A_{ij}\frac{\partial p}{\partial x_j}\right) + \nu \frac{\partial^2 |A|_F^2}{\partial x_k \partial x_k} - 2\nu \frac{\partial A_{ij}}{\partial x_k}\frac{\partial A_{ij}}{\partial x_k}, \quad (2.12)$$

which displays the favorable properties sought above.

First, $A_{ij}A_{ij} = S_{ij}S_{ij} + \Omega_{ij}\Omega_{ij}$, indicating that an integral measure based on the Frobenius norm of the velocity gradient tensor adds up the effects of both strain- and rotation-dominated regions, differentiating between the laminar and turbulent portions of a boundary layer. Second, unlike the viscous term in the Q equation, Eq. (2.9), the viscous dissipation term in Eq. (2.12) is associated with a negative sign and can, therefore, be interpreted clearly. Third, the pressure term in Eq. (2.12) is in divergence form, meaning that it can be neglected in the case of a zero-pressure-gradient flat-plate boundary layer due to the nominal scaling of pressure gradients in boundary layers. Finally, it is important to discuss the source term of Eq. (2.12), $A_{ik}A_{kj}A_{ij}$, and its physical meaning. $A_{ik}A_{kj}A_{ij}$ can be written as

$$A_{ik}A_{kj}A_{ij} = S_{ik}S_{kj}S_{ji} - \Omega_{ik}S_{kj}\Omega_{ji} = S_{ik}S_{kj}S_{ij} - \frac{1}{4}\omega_k S_{kj}\omega_j, \quad (2.13)$$

where ω_i is the vorticity in the ith direction. Equation (2.13) shows that the source term in the governing equation for $|A|_F^2$ can be decomposed into two contributions. First, $S_{ik}S_{kj}S_{ij}$ is the strain self-amplification term which contributes to the production of strain and can be shown to be negative on average by examining the term in its principal axes frame and noting that Ashurst *et al.* (1987) observed the positivity of the intermediate eigenvalue of the strain rate tensor. Second, $\omega_k S_{kj}\omega_j$ is the vortex stretching term leading to enstrophy production, which is on average positive due to both the preferential alignment of the vorticity vector with the intermediate eigenvector of the strain rate tensor and the axial vortex stretching due to the primary strain rate eigenvector, the latter being the dominant mechanism (Doan *et al.* 2018). Thus, on average, the source term of Eq. (2.12) is a positive quantity.

To proceed from Eq. (2.12), to an integral equation based on $\overline{|A|_F^2}$, we take the mean in the homogeneous spanwise direction and in time, noting that the boundary layer is statistically stationary. Then we integrate in the wall-normal direction across the boundary layer. This leads to the following equation

$$\begin{aligned} \frac{d}{dx}\left(\int_0^\infty \overline{u|A|_F^2}dy\right) = -2\int_0^\infty \overline{A_{ik}A_{kj}A_{ij}}dy - 2\frac{d}{dx}\left(\int_0^\infty \overline{\frac{\partial u}{\partial x_k}\frac{\partial p}{\partial x_k}}dy\right) \\ -\nu\frac{\partial \overline{|A|_F^2}}{\partial y}\bigg|_0 + \nu\frac{d^2}{dx^2}\left(\int_0^\infty \overline{|A|_F^2}dy\right) - 2\nu\int_0^\infty \overline{\frac{\partial A_{ij}}{\partial x_k}\frac{\partial A_{ij}}{\partial x_k}}dy, \end{aligned} \quad (2.14)$$

where both the pressure gradient term and the streamwise viscous term are kept for thoroughness, although we know that they are negligible on the basis of nominal boundary layer scaling. We will refer to these terms as, going from left to right, streamwise growth, gradient self-amplification, streamwise pressure transport, wall viscous deposition, streamwise viscous transport, and viscous destruction of velocity gradients.

The left-hand side of this equation can be thought of as the rate of change of the velocity gradient tensor magnitude as we march downstream along the boundary layer, in the frame of reference attached to the origin of the boundary layer. Thus, there is no time dependency due to statistical stationarity. As such, even though the left-hand side

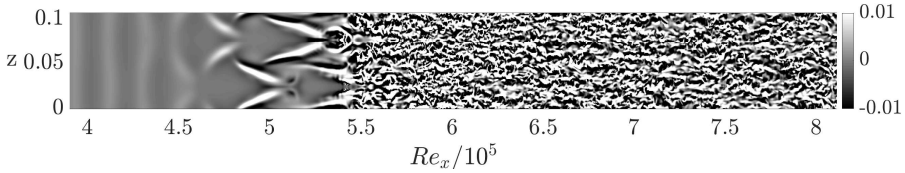

FIGURE 1. Wall-normal velocity at $y = 0.02\delta_{in}$.

of Eq. (2.14) is not Galilean invariant, it is only so because an average in time was taken, and in non-stationary flows, the addition of the time derivative would retrieve Galilean invariance. By observing the rapid generation of velocity gradients in a boundary layer around the transitional region, it is expected that the left-hand side term is small in both the laminar and fully turbulent regions of the boundary layer when compared to its magnitude during transition. In the fully turbulent region in the limit of high Reynolds numbers, the scaling presented by Tennekes & Lumley (1972) about the balance of enstrophy production and viscous dissipation suggests that the gradient self-amplification term and the viscous destruction term should be the dominant terms that balance in the $\overline{|A|_F^2}$ budget. By computing each of the terms on the right-hand side, we aim to identify the important mechanisms that drive transition through the generation of velocity gradients, as well as determine how far upstream this high Reynolds number scaling holds.

3. Numerical simulation

The numerical experiment follows a similar setup as the one presented by Lozano-Durán *et al.* (2018). In particular, it follows the case presented in Figure 1(b) of that paper, where the parabolized stability equations are used to march the initial boundary condition up to a matching location from which a DNS is carried out. The governing equations are integrated with a staggered second-order central finite-difference method, and time advancement utilized a second-order Runge-Kutta scheme combined with the fractional-step procedure. A zero-pressure-gradient flat-plate boundary layer is simulated as it undergoes H-type laminar-to-turbulent transition (Herbert 1988). Velocities are nondimensionalized using the free-stream velocity U_∞, and wall units are denoted by a superscript $+$ and defined in terms of the friction velocity u_τ and kinematic viscosity ν. Transition is triggered by imposing an inflow boundary condition that is the sum of the Blasius solution, a fundamental TS wave of nondimensional frequency $2F = \omega\nu/U_\infty^2$ and subharmonic mode of frequency F. These modes are the solution to the local Orr-Sommerfeld-Squire problem at $Re_x = 1.8 \times 10^5$.

Similarly to Lozano-Durán *et al.* (2018), the simulation box is periodic in the spanwise direction. It is narrower in the spanwise extent than in the cases presented by Lozano-Durán *et al.* (2018), and its size is equal to the inverse of the oblique wavenumber β associated with the subharmonic mode. Thus, there exists only a single Λ-vortex at any streamwise location in the simulation domain. Table 1 shows some of the important computational parameters, such as domain size, where δ_{in} indicates the initial boundary layer thickness at the Reynolds number corresponding to the matching location between PSE and DNS, $Re_{x,match}$.

Figure 1 shows a snapshot of the wall-normal velocity of the flow field, illustrating the staggered arrangement of Λ-vortices associated with H-type transition. Figure 2 shows

Δy^+_{min}	0.35
Δx^+	7.0
Δz^+	7.6
L_x	$142\delta_{in}$
L_y	$18\delta_{in}$
L_z	$6.5\delta_{in}$
δ_{out}/δ_{in}	≈ 3
$2F$	1.2395×10^{-4}
$\beta L_z/(2\pi)$	1.0078
$Re_{x,match}$	3.9×10^5

TABLE 1. Characteristic parameters of the simulation

the skin friction coefficient as a function of Re_x, along with the laminar and turbulent correlations, as well as the integral streamwise flux of the velocity gradients across the boundary layer as a function of Re_x. Even though the simulation domain is minimal in the spanwise extent, in the sense that we are enforcing the periodicity of each Λ-vortex, the skin friction coefficient displays the main features of controlled natural transition in larger domains, such as the skin friction overshoot (Sayadi *et al.* 2013). Furthermore, the profile of the integral streamwise flux of the velocity gradients across the boundary resembles the skin friction profile, indicating the rapid flux of velocity gradients around the transitional region. However, unlike the skin friction coefficient, this streamwise flux is not dependent on gradients at the wall.

3.1. *The* $|A|^2_F$ *budget*

To compute the terms in Eq. (2.14), 200 evenly spaced time instances spanning four periods of the TS wave were used. Figure 3 shows these terms as a function of Re_x. Figure 4 shows the same budget normalized by the gradient self-amplification as a function of Re_x and is truncated to start at $Re_x = 4.5 \times 10^5$ because that is the Reynolds number corresponding to the position when the gradient self-amplification term starts to become large. We can infer multiple things from Figures 3 and 4. First, consider the integral measure. Compared to its value around transition, its values in the laminar and turbulent regions are negligible, which matches our prior expectation and indicates that the largest changes in velocity gradients in a boundary are around the transition point. Second, consider the magnitudes of the gradient self-amplification and viscous destruction terms as compared to all the other terms in the budget. It is expected that at very high Reynolds numbers, these two terms should dominate the budget and match due to the same scaling arguments used to balance enstrophy production and viscous dissipation (Tennekes & Lumley 1972). This high Reynolds number scaling is apparent from Figure 4. However, it also extends back to the late stages of transition around $Re_x \approx 5.5 \times 10^5$, corresponding to the breaking of the Λ-vortices in Figure 1. This indicates that even at the late stages of transition, it is the same kinematic effects of vortex stretching and strain self-amplification that dominate the generation of large velocity gradients in the boundary layer.

This aforementioned result opens two avenues for further exploration. First, the study of models based on the Lagrangian dynamics of the velocity gradient tensor and their applicability in the transitional region could be explored, perhaps in the context of localized breakdown events. Second, the dynamics of the late stages of transition can be studied

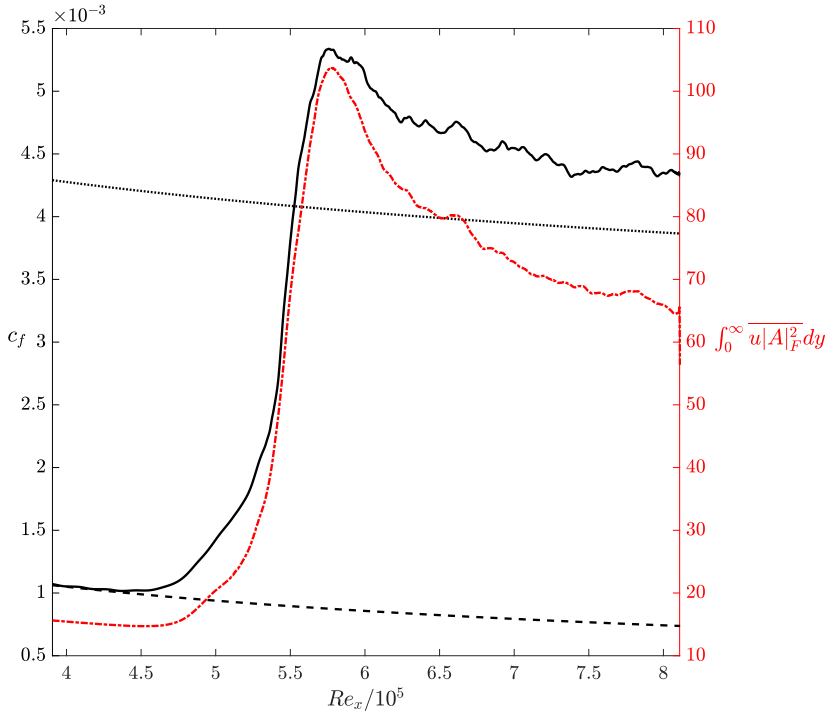

FIGURE 2. Left y-axis: Skin friction coefficient versus Re_x. —, H-type; ..., Blasius; - -, turbulent correlation (White 1974). Right y-axis: -.-, Integral streamwise flux of velocity gradients across the boundary layer versus Re_x.

to formulate reduced-order dynamical models that are applicable at the fully developed turbulent regions of the boundary layer (Sayadi *et al.* 2013). This second approach could be pursued from the perspective of coherent structures and has been explored by Sayadi *et al.* (2014) using dynamic mode decomposition.

It is important to note that only qualitative results were inferred from Figures 3 and 4, due to the two sides of Eq. (2.14) not balancing numerically. However, in the region of interest $Re_x \geqslant 4.5 \times 10^5$, the relative magnitude of the difference between the left- and right-hand sides of the equation is approximately 8% when compared to the largest term in the budget, the gradient self-amplification term. This difference is expected for several reasons. First, Eq. (2.14) holds in a continuous sense, and as such, we do not expect the two sides of the equation to balance unless it was derived discretely. Second, Eq. (2.14) is valid for a statistically stationary flow, and the minor oscillations still present in the budget indicates that further averaging is required to warrant neglecting the time derivative on the left-hand side. Third, and more importantly, the terms present in Eq. (2.14) include higher-order derivatives, such as the viscous destruction term, that require high-order numerical schemes, as well as higher resolution, to be accurately captured (Lozano-Durán *et al.* 2015, 2016). Taking these limitations into account, the qualitative statements made can still be justified.

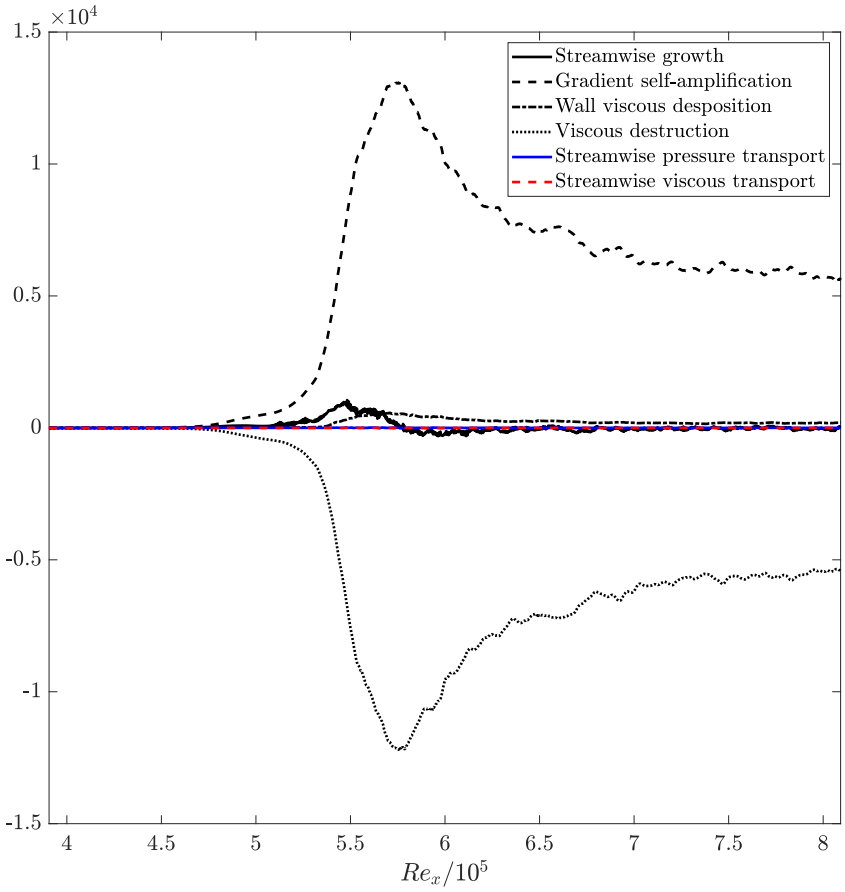

FIGURE 3. Eulerian budget of the Frobenius norm of the velocity gradient tensor, Eq. (2.14), versus Re_x.

4. Conclusions

In this report, we study the transition to turbulence from the perspective of the velocity gradient tensor dynamics. Our work is motivated by the observation of nonlinear structures emerging during transition, as revealed by vortex identifiers such as the Q-criterion. To that end, we have derived transport equations based on several invariants of the velocity gradient tensor to obtain integral budgets spanning the different stages of transition from laminar to turbulent flow. We have also discussed which quantity would be the most appropriate in our study, while keeping in mind the potential for future modeling applications.

The Frobenius norm of the velocity gradient tensor, $|A|_F^2$, was identified as a suitable marker for transition due to the independence of its growth from the pressure term. It was found that the source term for $|A|_F^2$, which was a combination of the vorticity stretching and strain self-amplification mechanisms, is balanced by the viscous destruc-

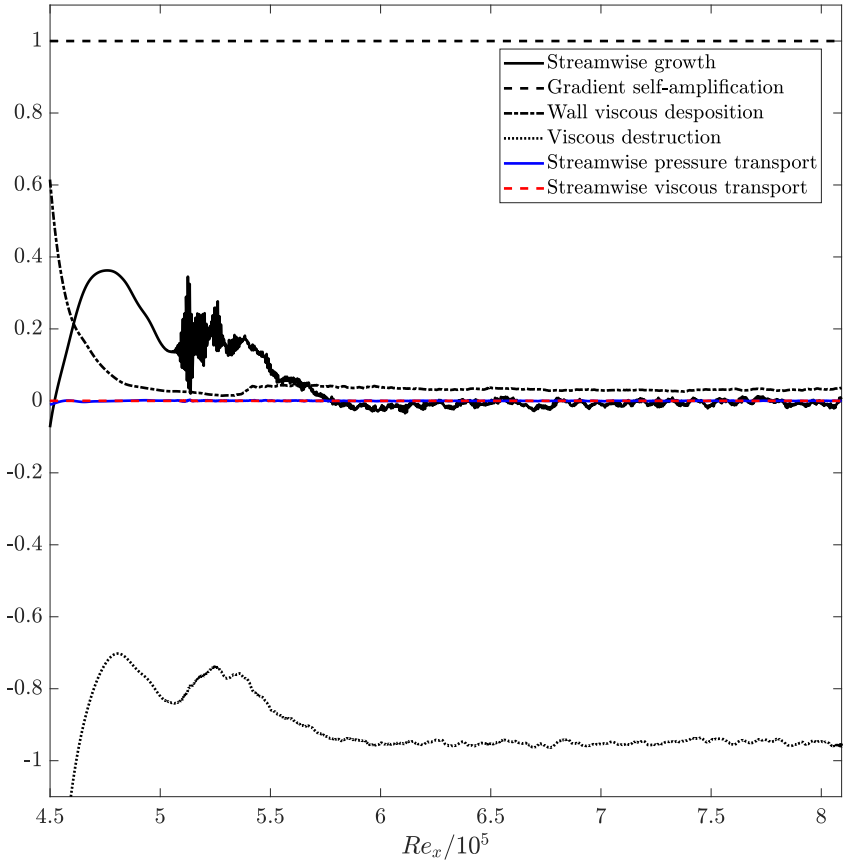

FIGURE 4. Eulerian budget of the Frobenius norm of the velocity gradient tensor, Eq. (2.14), normalized by the gradient self-amplification term versus Re_x.

tion/dissipation term, and that the two terms are at least one order of magnitude larger than the remaining terms in the integral budget. This result, already documented at the high Reynolds number turbulence, was also found to hold at the late stages of transition associated with the initial breakup of the Λ-vortices. The outcome suggests that some of the dynamics that govern fully developed turbulence are also present in the late stages of transition, and that these late-stage dynamics might aid the development of reduced-order models for fully developed turbulence. At the same time, it provides support to the study of transition from the point of view of Lagrangian velocity gradient tensor dynamics.

Acknowledgments

P.L.J. was funded by the Advanced Simulation and Computing (ASC) program of the US Department of Energy's National Nuclear Security Administration via the PSAAP-

II Center at Stanford, Grant No. DE-NA0002373. A.L.-D. acknowledges the support of NASA under grant No. NNX15AU93A and of ONR under grant No. N00014-16-S-BA10.

REFERENCES

Ashurst, W. T., Kerstein, A. R., Kerr, R. M. & Gibson, C. H. 1987 Alignment of vorticity and scalar gradient with strain rate in simulated Navier-Stokes turbulence. *Phys. Fluids* **30**, 2343–2353.

Cantwell, B. J. 1992 Exact solution of a restricted Euler equation for the velocity gradient tensor. *Phys. Fluids A* **4**, 782–793.

Chertkov, M., Pumir, A. & Shraiman, B. I. 1999 Lagrangian tetrad dynamics and the phenomenology of turbulence. *Phys. Fluids* **11**, 2394–2410.

Chevillard, L. & Meneveau, C. 2006 Lagrangian dynamics and statistical geometric structure of turbulence. *Phys. Rev. Lett.* **97**, 174501.

Chevillard, L., Meneveau, C., Biferale, L. & Toschi, F. 2008 Modeling the pressure Hessian and viscous Laplacian in turbulence: Comparisons with direct numerical simulation and implications on velocity gradient dynamics. *Phys. Fluids* **20**, 101504.

Doan, N. A., Swaminathan, N., Davidson, P. A. & Tanahashi, M. 2018 Scale locality of the energy cascade using real space quantities. *Phys. Rev. Fluids* **3**, 84601.

Herbert, T. 1988 Secondary instability of boundary layers. *Ann. Rev. Fluid Mech.* **20**, 487–526

Lozano-Durán, A., Hack, M. J. P. & Moin, P. 2018 Modeling boundary-layer transition in direct and large-eddy simulations using parabolized stability equations. *Phys. Rev. Fluids* **3**, 23901.

Lozano-Durán, A., Holzner, M. & Jiménez, J. 2015 Numerically accurate computation of the conditional trajectories of the topological invariants in turbulent flows. *J. Comput. Phys.* **295**, 805–814.

Lozano-Durán, A., Holzner, M. & Jiménez, J. 2016 Multiscale analysis of the topological invariants in the logarithmic region of turbulent channels at a friction Reynolds number of 932. *J. Fluid Mech.* **803**, 356–394.

Mack, LM. 1984 Boundary-layer linear stability theory. In Special Course on Stability and Transition of Laminar Flow. *AGARD Rep. No. 709*, Part 3, pp. 1–81.

Meneveau, C. 2011 Lagrangian dynamics and models of the velocity gradient tensor in turbulent flows. *Ann. Rev. Fluid Mech.* **43**, 219–245.

Sayadi, T., Hamman, C. W. & Moin, P. 2013 Direct numerical simulation of complete H-type and K-type transitions with implications for the dynamics of turbulent boundary layers. *J. Fluid Mech.* **724**, 480–509.

Sayadi, T., Schmid, P. J., Nichols, J. W. & Moin, P. 2014 Reduced-order representation of near-wall structures in the late transitional boundary layer. *J. Fluid Mech.* **748**, 278–301.

Schmid, P. J. & Henningson, D. S. 2001 *Stability and Transition in Shear Flows*. Springer.

Soria, J., Sondergaard, R., Cantwell, B. J., Chong, M. S. & Perry, A. E. 1994 A study of the fine-scale motions of incompressible time-developing mixing layers. *Phys. Fluids* **6**, 871–884.

Tennekes, H. & Lumley, J. L. 1972 *A First Course in Turbulence*. MIT Press.

Vieillefosse, P. 1982 Local interaction between vorticity and shear in a perfect incompressible fluid. *J. Phys. Paris* **43**, 837–842.

White, F. M. 1974 *Viscous Fluid Flow*. McGraw-Hill.

Wu, X., Moin, P., Wallace, J. M., Skarda, J., Lozano-Durán, A. & Hickey, J.-P. 2017 Transitional–turbulent spots and turbulent–turbulent spots in boundary layers. *Proc. Natl. Acad. Sci.* **114**, E5292.